Applied Mathematics & Information Sciences
An International Journal

http://dx.doi.org/10.18576/amis/160621

Peristaltic Transport of Fractional Jeffrey Fluid in a Nonuniform Channel: Role of heat transfer

H. S. Gafel

Department of Mathematics and Statistics, College of Science, Taif University, P.O. Box 11099, Taif 21944, Saudi Arabia

Received: 2 Jul. 2022, Revised: 2 Sep. 2022, Accepted: 12 Oct. 2022.
Published online: 1 Nov. 2023.

Abstract: This article's goal is to explain how heat transfer affects the peristaltic movement of the fractional Jeffrey fluid over a permeable media in a non-uniform channel. The consequences of fractional viscoelastic properties of the generalized Jeffrey fluid are explored together with the effects of heat transfer, geometric features of the non-uniform channel, and peristaltic flow. There is a visual comparison between the two. By means of the suppositions of a long wavelength, the analytical solutions of the velocity, pressure gradient, and pressure rise are inspected. According to the data, the permeability, Grashof number, wave amplitude, heat source, thermal radiation, and thermal slip all have a significant impact on the phenomenon. Additionally, a comparison of the results of an analytical solution with earlier literature demonstrates satisfactory agreement.

Keywords: Peristaltic flow, Fractional Maxwell fluid, Viscoelastic fluid, porous medium, Heat transfer.

Nomenclature

b	amplitude
$a(x)$	channel's half-width
a_o	The half width of the inlet of the channel
m	Constant whose value relies on the width and depth of the inlet and exit as well as the length of the channel
λ	Wavelength
$\bar{u}, \bar{v}$	Velocity components
K	Permeability
q_r	Radiative heat flux
K_1	The thermal conductivity
$\bar{Q}$	Heat generation coefficient
θ	Temperature distribution
η	The porosity of the porous medium
$\bar{D}_{\bar{t}}^{\alpha_1}, \bar{D}_{\bar{t}}^{\beta_1}$	The fractional calculus of order α_1 and β_1
α_1, β_1	Fractional time derivative parameters

1 Introduction

Peristalsis is the constant wavelike muscular reduction of hollow tubes and biological vessels, for example, the esophagus, stomach, intestines, occasionally the ureters, and blood vessels. Peristaltic transport describes the movement of fluids by peristalsis. Khan et al. [1] have researched peristaltic motion in both mechanical and physiological contexts. The effects of fractional Maxwell fluids on peristaltic flows were evaluated by Bayones et al. [2]. The impact of the endoscope and on the peristaltic flow was noted by Abd-Alla et al. [3]. Asjad et al. [4] deliberated the flow of unstable MHD viscous fluid including carbon nanotubes (SWCNTs, MWCNTs) nanoparticles and using carboxymethyl cellulose (CMC) as its base fluid. Mainardi and Spada [5] examined the fundamental fractional models. Qi and Jin [6] proposed the unstable rotational flows of a viscoelastic fluid between consecutive cylinders. The algorithmic strategy for the unstable flow of a Maxwell fluid with Caputo variable coefficients was explored by Haque et al. [7]. Carrera et al. [8] demonstrated the Maxwell model for non-Newtonian fluids. The new model was used by Tripathi and colleagues [9] to illustrate the peristalsis-based movement of a viscoelastic fluid via a conduit. Guo et al. [10] demonstrated the fractional Jeffrey fluid's model. Also, another fractional Maxwell model was used by Tripathi [11]. Peristaltic pump phenomena were premeditated by Abd-Alla et al. [12]. Guo and Qi [13] investigated the electrical peristaltic flow of a viscous fluid. Narla et al. [14] were able to precisely determine the analytical solutions for the flow of a viscoelastic fluid down a rounded channel. Razzaq et al. [15] calculated the heat transport analysis of a fractional Maxwell fluid. Some recent study on this subject is covered in [16–25].

In this study, we investigate the fractional Maxwell model-based peristaltic transportation of viscoelastic Newtonian Jeffery fluid along a porous channel underneath the long wavelength and low Reynolds number preconceptions. We have talked about the implications of permeability and fractional time derivative factors. The constant whose size is determined by the channel length and the magnitudes of the inlet and outlet, the Grashof number wave amplitude, the heat source, the thermal radiation, the ratio of relaxation

*Corresponding author e-mail: h.gafal@tu.edu.sa

to retardation times the retardation period, and the current findings offer a fundamental comprehension of the physical model in addition to being helpful for practical applications.

2 Formulation of the Problem

The Jeffrey model's fundamental relationship for an incompressible fluid is as follows:

$$T = -PI + S, \tag{1}$$

$$\overline{S}\left(1+\overline{\lambda_1}^{\alpha_1}\widetilde{D}_t^{\alpha_1}\right)=\mu A, \tag{2}$$

The upper convicted fractional derivative is given by:

$$\widetilde{D}_t^{\alpha_1}(\overline{S}) = D_t^{\alpha_1}(\overline{S}) + (\overline{V}.\nabla)(\overline{S}) - \overline{L}(\overline{S}) - (\overline{S})\overline{L}^T \tag{3}$$

In which

$$A = (\nabla\overline{V}) + (\nabla\overline{V})^T \tag{4}$$

$$D_t^{\alpha_1} f(t) = \frac{1}{\Gamma(1-\alpha_1)}\frac{d}{dt}\int_0^t \frac{f(\xi)}{(t-\xi)^{\alpha_1}}d\xi, \qquad 0\le\alpha_1\le 1. \tag{5}$$

Here, $\Gamma(.)$ represents the gamma function.

$A = \overline{L} + \overline{L}^T$, is termed as the main Rivlin-Ericksen tensor, $L = \nabla\overline{V}$ is defined as the velocity gradient, and $\overline{V}$ is the velocity vector.

The crucial relationship of the classical Jeffrey fluid gives the correlation existed of the fractional Jeffrey fluid:

$$\overline{S}\left(1+\overline{\lambda_1}^{\alpha_1}D_t^{\alpha_1}\right)=\mu A\left(1+\overline{\lambda_2}^{\beta_1}D_t^{\beta_1}\right). \tag{6}$$

We consider fractional Jeffrey fluid peristalsis via a permeable channel through the parallel to the middle line and perpendicular to it (Figure 1). The geometry of the wave-propagating tube walls is given by:

$$Y_f = \pm H = \pm\left[a\left(\overline{X_f}\right)+b\sin\left(\frac{2\pi}{\lambda}\left(\overline{X_f}-c\overline{t_f}\right)\right)\right], \tag{7}$$

The governing equations of the flow viscoelastic fluid in a porous medium are as follows:

$$\rho\left[\frac{\partial\overline{U_f}}{\partial\overline{t_f}}+\overline{U_f}\frac{\partial\overline{U_f}}{\partial\overline{X_f}}+\overline{V_f}\frac{\partial\overline{U_f}}{\partial\overline{Y_f}}\right]=-\frac{\partial\overline{P_f}}{\partial\overline{X_f}}+\frac{\partial\overline{S}_{\overline{X_f}\overline{X_f}}}{\partial\overline{X_f}}+\frac{\partial\overline{S}_{\overline{X_f}\overline{Y_f}}}{\partial\overline{Y_f}} + \rho g\overline{\alpha_t}\left(\overline{T}-T_0\right)+r, \tag{8}$$

$$\rho\left[\frac{\partial\overline{V_f}}{\partial\overline{t_f}}+\overline{U_f}\frac{\partial\overline{V_f}}{\partial\overline{X_f}}+\overline{V_f}\frac{\partial\overline{V_f}}{\partial\overline{Y_f}}\right]=-\frac{\partial\overline{P_f}}{\partial\overline{Y_f}}+\frac{\partial\overline{S}_{\overline{X_f}\overline{Y_f}}}{\partial X_f}+\frac{\partial\overline{S}_{\overline{Y_f}\overline{Y_f}}}{\partial Y_f}, \tag{9}$$

$$\rho_{Cp}\left[\frac{\partial\overline{T_f}}{\partial\overline{t_f}}+\overline{U_f}\frac{\partial\overline{T_f}}{\partial\overline{X_f}}+\overline{V_f}\frac{\partial\overline{T_f}}{\partial\overline{Y_f}}\right]=K_1\left(\frac{\partial^2\overline{T_f}}{\partial\overline{X_f}^2}+\frac{\partial^2\overline{T_f}}{\partial\overline{Y_f}^2}\right) - \frac{\partial q_r}{\partial\overline{Y}}+\overline{Q}, \tag{10}$$

$$\frac{\partial\overline{U_f}}{\partial\overline{X_f}}+\frac{\partial\overline{V_f}}{\partial\overline{Y_f}}=0. \tag{11}$$

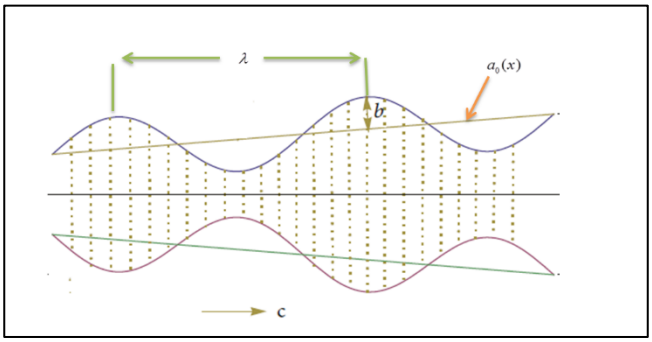

Fig. 1: The problem's geometry.

This Darcy resistance r is apparent from the equation (8) that satisfies the formula:

$$r\left(1+\overline{\lambda_1}^{\alpha_1}\overline{D_t}^{\alpha_1}\right)=\frac{-\mu\eta}{\overline{K}}\left(1+\overline{\lambda_1}^{\beta_1}\overline{D_t}^{\beta_1}\right)\overline{V}. \tag{12}$$

where, $(\overline{K}>0)$ and $(0<\eta<1)$ is porosity of the porous medium. The changes between the two frames are assumed by:

$$\overline{x} = \overline{X_f} - c\overline{t_f},\ \overline{p} = \overline{P_f},\ \overline{y} = \overline{Y_f},$$
$$\overline{v} = \overline{V_f},\ \overline{u} = \overline{U_f} - c,\ \overline{T_f} = T. \tag{13}$$

The pertaining boundary conditions are as follows:

$$\frac{\partial\overline{U_f}}{\partial\overline{Y_f}} = 0 \quad at \quad \overline{Y_f} = 0,$$
$$\overline{U_f} = 0 \quad at \quad \overline{Y_f} = H, \tag{14}$$

$$\overline{T_f}+\gamma\frac{\partial\overline{T_f}}{\partial\overline{Y}}=T_0 \quad at \quad \overline{Y_f}=+H,$$

$$\overline{T_f}+\gamma\frac{\partial\overline{T_f}}{\partial\overline{Y_f}}=T_1 \quad at \quad \overline{Y_f}=-H, \tag{15}$$

$$\frac{\partial\overline{P_f}}{\partial\overline{X_f}}=0 \quad at \quad \overline{Y_f}=0. \tag{16}$$

The non-dimensional variables include the following:

$$x=\frac{\bar{x}}{\lambda},\ y=\frac{\bar{y}}{a_0},\ u=\frac{\bar{u}}{c},\ v=\frac{\bar{v}}{c\delta},$$

$$t=\frac{c\bar{t}}{\lambda},\ h_1=\frac{\overline{H_1}}{a_0},\ h_2=\frac{\overline{H_2}}{a_0},\ \lambda_1=\frac{c\overline{\lambda_1}}{\lambda},$$

$$\lambda_2=\frac{c\overline{\lambda_2}}{\lambda},\ \delta=\frac{a_0}{\lambda},\ p=\frac{{a_0}^2\overline{p}}{c\lambda\mu},\ K=\frac{\overline{K}}{\eta{a_0}^2},$$

$$\phi=\frac{b}{a_0},\ \mathrm{Pr}=\frac{\mu c_P}{K_1},\ \mathrm{Re}=\frac{\rho c a_0}{\mu},$$

$$Gr=\frac{\rho g\overline{\alpha_t}(T_1-T_o){a_o}^2}{\mu c},\ \beta=\frac{{a_0}^2\overline{Q}}{K_1(T_1-T_o)},$$

$$R=\frac{16\overline{\sigma}{T_0}^3}{3\overline{k}K_1},\ \theta=\frac{\overline{T}-T_0}{T_1-T_0}. \tag{17}$$

The radiative flux q_r of radiation is sculpted as follows:

$$q_r=-RK_1\frac{\partial\overline{T}}{\partial\overline{y}}. \tag{18}$$

Volume flow rate F, pressure rise ΔP_λ, and frictional forces' respective non-dimensional expressions are produced by:

$$F=\int_0^h udy \tag{19}$$

$$\Delta P_\lambda=\int_0^1\left(\frac{dp}{dx}\right)dx \tag{20}$$

$$F_\lambda=\int_0^1 h\left(-\frac{dp}{dx}\right)dx \tag{21}$$

3 Solution of the Problem

By means of the dimensionless amounts mentioned above and assuming the long-wavelength approximation and low Reynolds numbers, the equations of motion assume the following form:

$$\left(1+\lambda_1^{\alpha_1}\partial_t^{\alpha_1}\right)\left[\frac{dp}{dx}-Gr\theta\right]=\left(1+\lambda_1^{\beta_1}\partial_t^{\beta_1}\right)\left[\frac{\partial^2u}{\partial y^2}-\frac{1}{K}(u+1)\right], \tag{22}$$

$$\frac{\partial p}{\partial y}=0, \tag{23}$$

$$(1+R)\frac{\partial^2\theta}{\partial y^2}+\beta=0. \tag{24}$$

The following formulas for temperature distribution, velocity, and pressure gradient can be attained:

$$\theta=\frac{1}{2}\left(1-\frac{y}{h+\gamma}+k\left(h^2-y^2+2h\gamma\right)\right), \tag{25}$$

$$u=q_1\times\left(q_2+q_3+q_4+q_5\right), \tag{26}$$

$$\frac{dp}{dx}=\frac{F-Z_1}{Z_2}. \tag{27}$$

where,

$$S_1=-\frac{b_2}{b_1}, \tag{28}$$

$$S_2=-\frac{\left(b_3+b_4+b_5\right)}{b_1}. \tag{29}$$

The equations (32) –(35) contain expressions for the unknowns $q_1,q_2,q_3,q_4,q_5,$

$b_1,b_2,b_3,b_4,b_5,Z_1,Z_2,k,$ Given in the Appendix

4 Numerical Results and Discussion

Numerous values of the fractional Maxwell fluid, fractional time derivative parameters, α_1 and β_1, permeability K, Grashof number Gr, wave amplitude, ϕ, heat source β, thermal radiation R, thermal slip γ, the ratio of relaxation to retardation times λ_1, retardation time λ_2, and the dimensions of the inlet and exit were numerically calculated in order to analyze the behavior of solutions.

Figure 2 illustrates the temperature fluctuations with regard to distance y for various physical thermal radiation parameters, including R, β, γ and ϕ. It has been noted that an increase in R values results in temperature drops over $-1 \le y \le -0.6,$ while it causes increases in temperature in the interval $-0.6 \le y \le 0.83,$ as well it increases with increasing of heat source/sink in the interval $-1 \le y \le -0.6,$ while it declines with increasing of β in the interval $-0.6 \le y \le 0.83,$ otherwise with the increases in γ and ϕ cause the reduction in temperature. In addition, the temperature dropped as the axis was increased, and the boundary criteria were met.

The pressure gradient $\frac{dp}{dx}$ is plotted against $x \in [0,1)$ in **figure 3** for different values of α_1, β_1, K, Gr, ϕ, β, $R,$ and γ. Noting that the peristaltic motion is what causes the pressure gradient to oscillate, we can see that it has done so across the entire range of axes. It decreases with the increasing of β_1, $K,$ and $Gr,$ while it increases with the increasing of α_1. Otherwise it declines with the increasing of ϕ in the interval $x \in [0,1)$ and it \increases with the increasing of wave amplitude ϕ in the interval $x \in (0.5,1).$ As well as increasing and decreasing of β, $R,$ and γ in the complete range of $x-$ axis. It is obvious that growing thermal slip and thermal radiation exhibit oscillatory behavior due to peristaltic motion [26], as we can realize, they have oscillated across the whole axis range.

Figure 4 is plotted for various values of α_1 and β_1, λ_1, and λ_2, It is perceived that the pressure rise Δp_λ rises rapidly with the increase of α_1 and λ_2 when $F \in (-300,0),$ while it decreases when $F \in (0,300),$ while the it declines with increasing of β_1, and λ_1, when $F \in (-300,0),$ as well it increases when $F \in (0,300).$ As anticipated, pressure rise results in higher values for small volume flow rates and smaller values for large volume flow rates. Furthermore, peristaltic pumping arises in the region where augmented pumping would otherwise occur.

Figure 5 clarifies the variation of frictional force F_λ against volume flow rate F for different values of α_1 and β_1, ϕ, and $m.$ It is detected that there is a direct relative between frictional force and volume flow rate, i.e. the frictional force increases by increasing β_1, ϕ, and $m.$ when $F \in (0,300),$ while it declines when $F \in (-300,0),$ in addition it falls by increasing α_1 when $F \in (-300,0),$ while it increases when $F \in (0,300).$ when compared to that pressure rise, the frictional force similarly behaves in the opposite way. This outcome is comparable to that shown in reference [25].

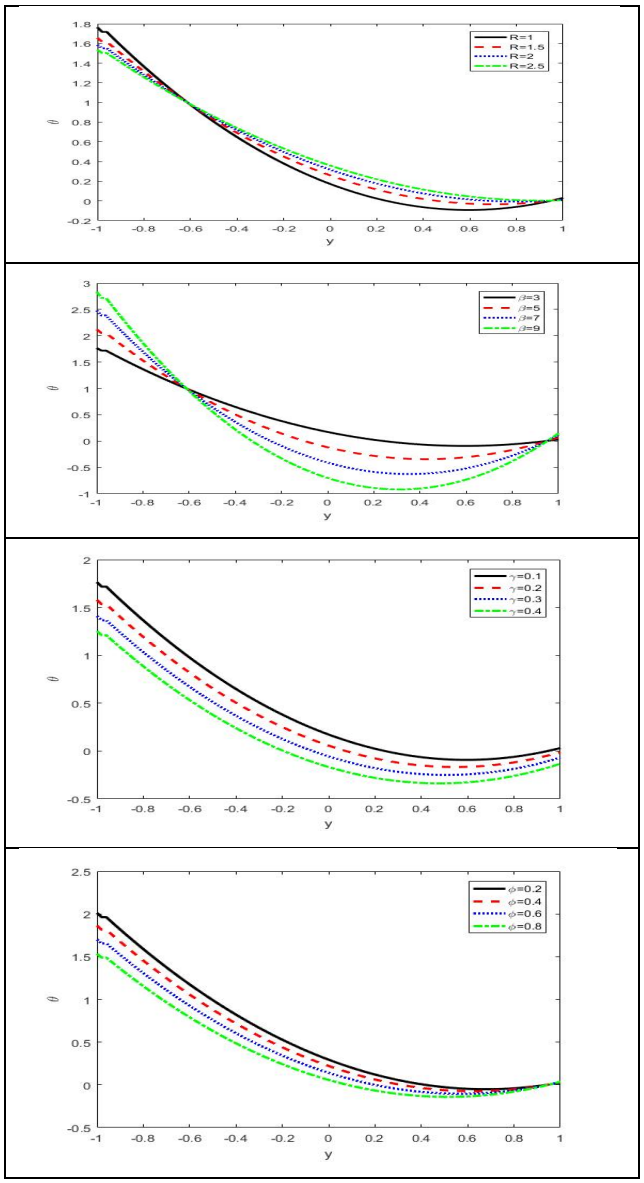

Fig. 2: The dissimilarities of the temperature θ.

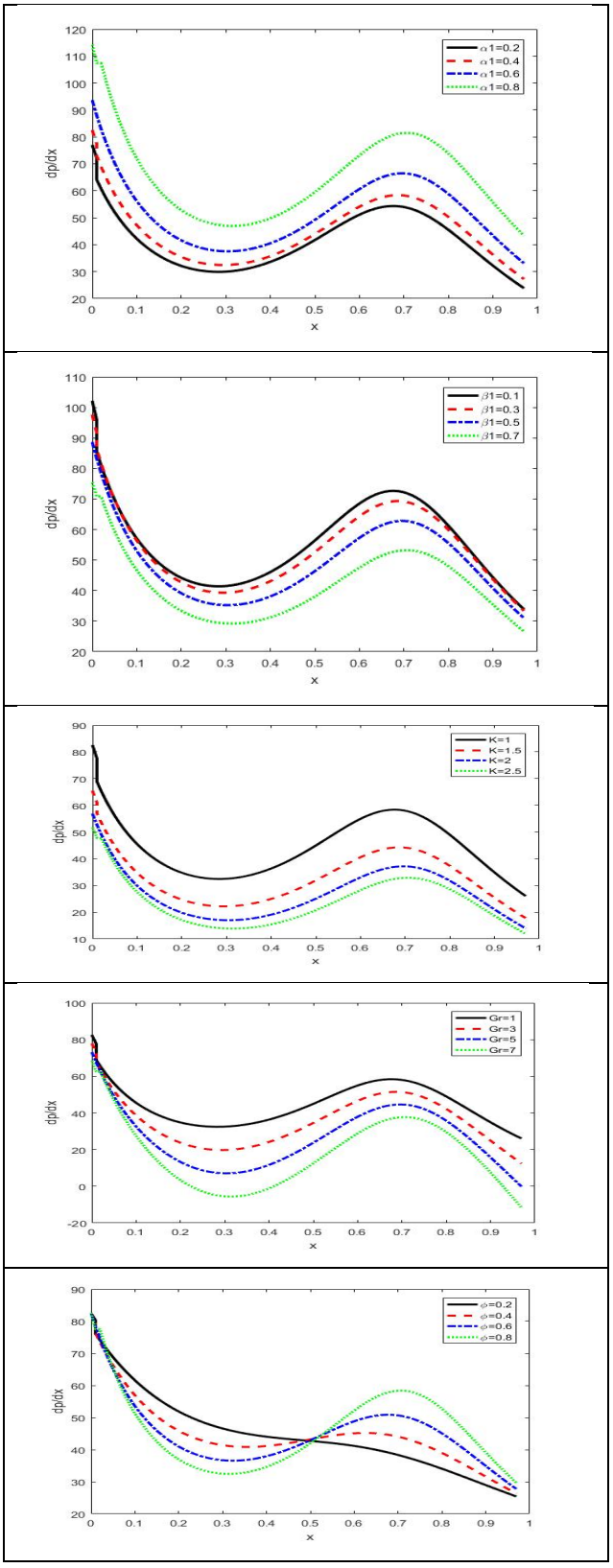

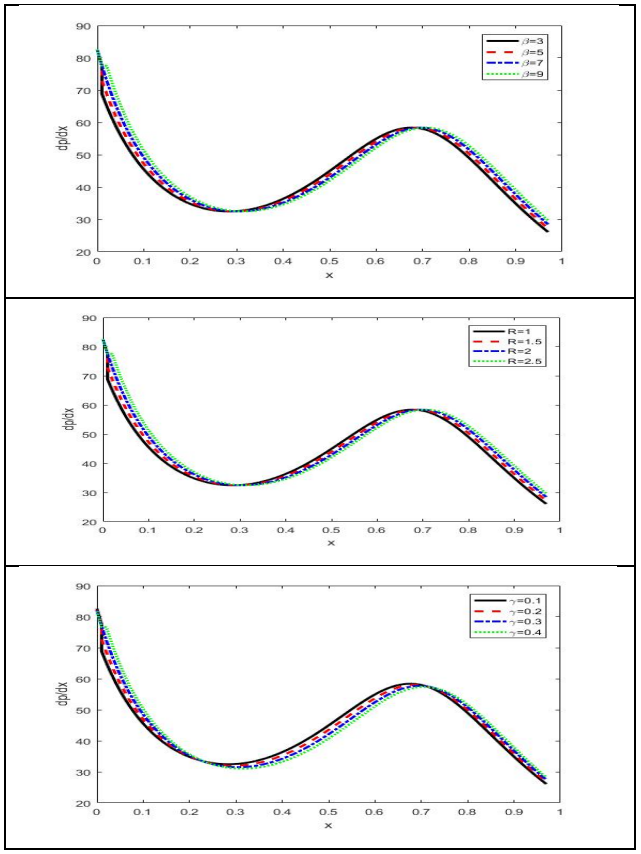

Fig. 3: The dissimilarities of the pressure gradient $\frac{dp}{dx}$.

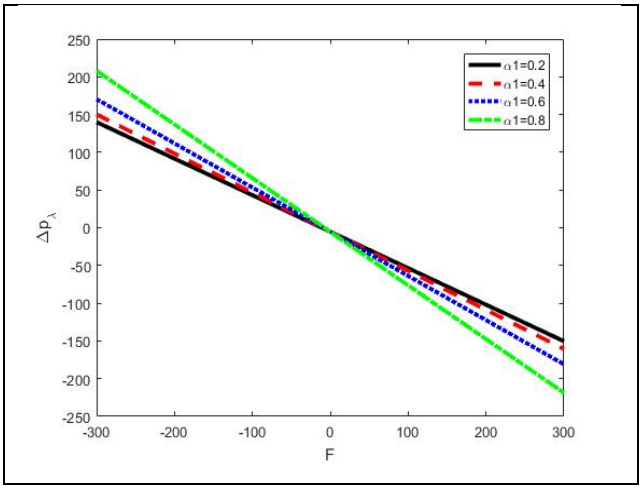

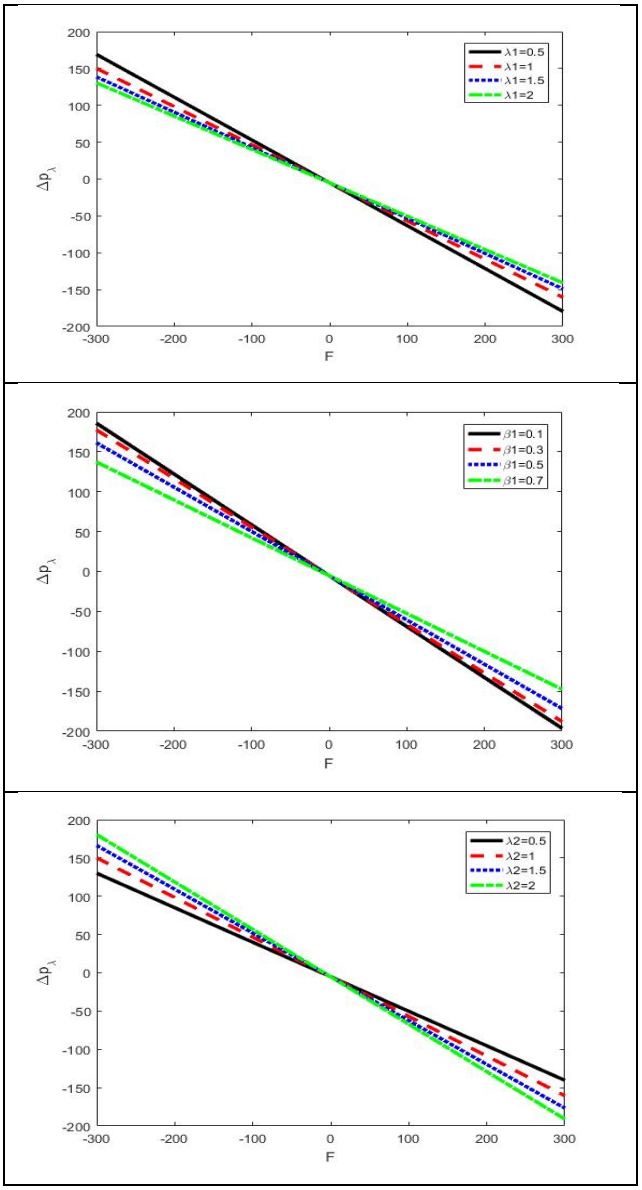

Fig. 4: The dissimilarities of the pressure rise Δp_λ.

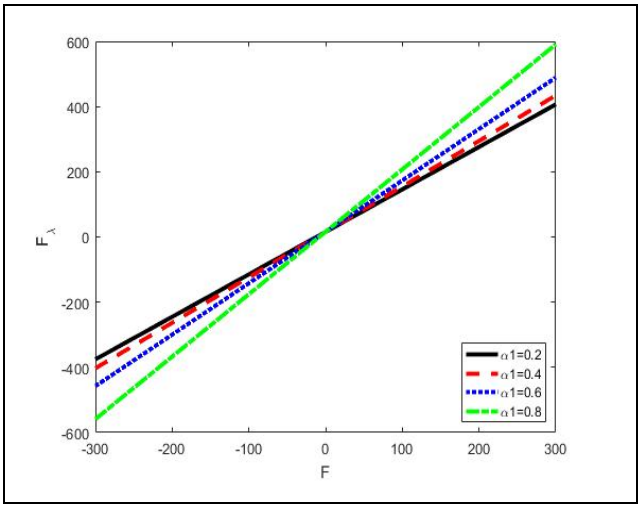

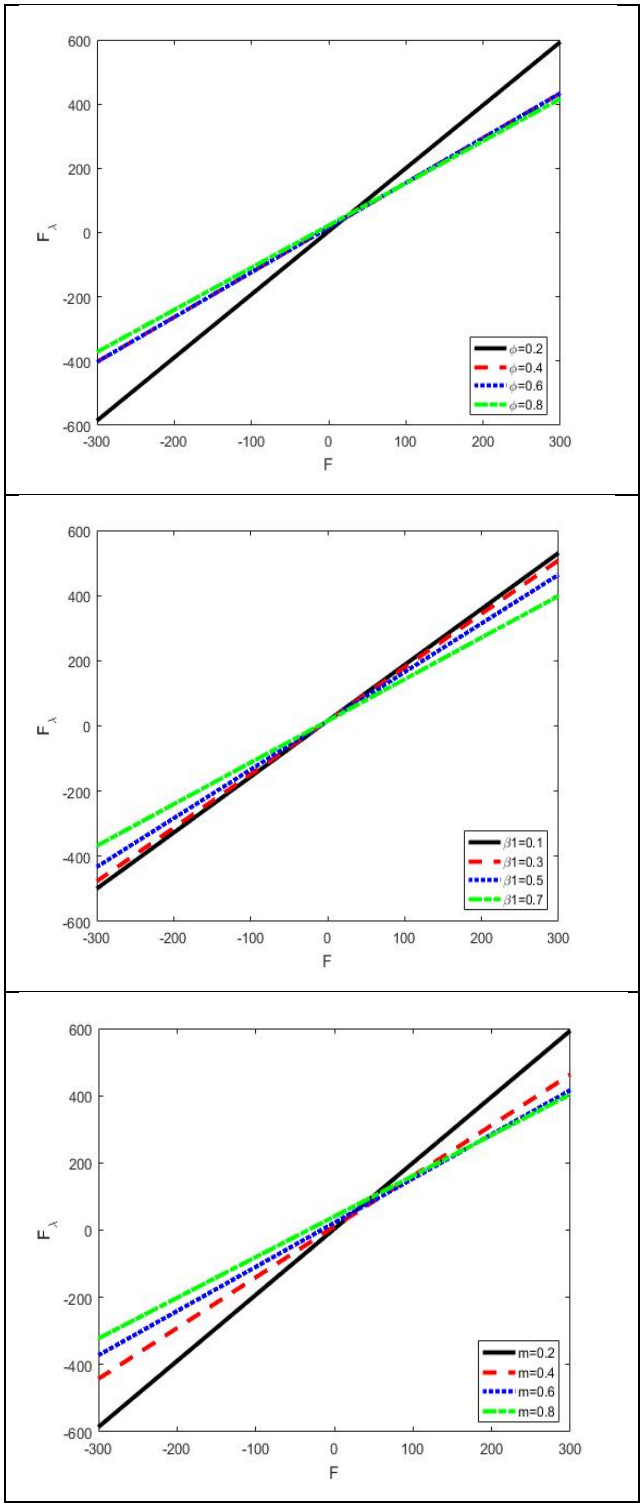

Fig. 5: The dissimilarities of the friction forces F_λ.

5 Conclusions

Since it uses derivatives and integrals, fractional calculus is a natural generalization of classical calculus. Although the idea of fractions seems strange, it has recently drawn the attention of scientists and researchers and has shown to be

an effective and popular tool for managing numerous physical processes in numerous branches of engineering and science. This study presents the impact of the peristaltic flow of the fractional Jeffrey fluid with heat transfer through a porous media in a non-uniform channel. Within long-wavelength and low Reynolds number approximations, the effects of Hartman number, the fractional Maxwell fluid, and heat transfer on the peristaltic flow of a Jeffrey fluid through a medium were assessed. For the variables of temperature, axial velocity, and pressure gradient, analytical solutions were created. The results of this investigation can be summed up as follows:

1- Temperature decreases as thermal slip and phase difference grow while all other factors remain constant.

2- The scale of $\frac{dp}{dx}$ decreases when there is an increase in fractional time derivative parameter, permeability and Grashof number.

3- The results of this study should be useful to researchers in the domains of science, medicine, engineering, and fluid mechanics.

Appendix

$$k=\frac{-\beta}{1+R},$$

$$f_1=\left(1+\lambda_1{}^{\alpha_1}\partial_t^{\alpha_1}\right),\qquad f_2=\left(1+\lambda_1{}^{\beta_1}\partial_t^{\beta_1}\right),$$

$$q_1=\frac{e^{\frac{-y}{\sqrt{K}}}}{2\left(1+e^{\frac{2h}{\sqrt{K}}}\right)f_2(h+\gamma)},$$

$$q_2=-e^{\frac{2h}{\sqrt{K}}}f_1GrK^{\frac{3}{2}}+e^{\frac{2y}{\sqrt{K}}}f_1GrK^{\frac{3}{2}}+e^{\frac{h}{\sqrt{K}}}\left(2f_2(h+\gamma)+f_1K\left(2\frac{dp}{dx}(h+\gamma)-Gr\left(\gamma+2k(h+\gamma)(-k+h\gamma)\right)\right)\right),$$

$$q_3=-e^{\frac{h+2y}{\sqrt{K}}}\left(2f_2(h+\gamma)+f_1K\left(2\frac{dp}{dx}(h+\gamma)-Gr\left(\gamma+2k(h+\gamma)(-k+h\gamma)\right)\right)\right),$$

$$q_4=-e^{\frac{2h+y}{\sqrt{K}}}\left(-2f_2(h+\gamma)+f_1K\left(2\frac{dp}{dx}(h+\gamma)-Gr\left(\begin{matrix}-kh^3+y-3kh^2\gamma+\\(-1+2kK+ky^2)\gamma+h\left(-1+k(2K+y^2-2\gamma^2)\right)\end{matrix}\right)\right)\right),$$

$$q_5=-e^{\frac{y}{\sqrt{K}}}\left(2f_2(h+\gamma)+f_1K\left(2\frac{dp}{dx}(h+\gamma)+Gr\left(\begin{matrix}-kh^3+y-3kh^2\gamma+\\(-1+2kK+ky^2)\gamma+h\left(-1+k(2K+y^2-2\gamma^2)\right)\end{matrix}\right)\right)\right),$$

$$b_1=2\left(1+e^{\frac{2h}{\sqrt{K}}}\right)f_2(h+\gamma),$$

$$b_2=4e^{\frac{h}{\sqrt{K}}}f_1hK(h+\gamma)\cosh\left(\frac{h}{\sqrt{K}}\right)-4e^{\frac{h}{\sqrt{K}}}f_1K^{\frac{3}{2}}(h+\gamma)+\sinh\left(\frac{h}{\sqrt{K}}\right),$$

$$b_3=-2e^{\frac{h}{\sqrt{K}}}f_1GrK^2+2f_2\left(h+e^{\frac{2h}{\sqrt{K}}}(h-\sqrt{K})+\sqrt{K}\right)(h+\gamma)+2^{\frac{h}{\sqrt{K}}}f_1GrK^2\cosh\left(\frac{h}{\sqrt{K}}\right),$$

$$b_4=-\frac{1}{3}e^{\frac{h}{\sqrt{K}}}f_1GrhK_2\left(h\left(3+4k(h^2-3K)\right)+2(3+8kh^2-6kK)\gamma++12kh\gamma^2\right)\cosh\left(\frac{h}{\sqrt{K}}\right),$$

$$b_5=2e^{\frac{h}{\sqrt{K}}}f_1GrK^{\frac{3}{2}}\left(\gamma+2k(h+\gamma)(-k+h\gamma)\right)\sinh\left(\frac{h}{\sqrt{K}}\right).$$

Conflict of interest

The authors declare that there is no conflict regarding the publication of this paper.

References

[1] A. Khan, D. Khan, I. Khan, M. Taj, I. Ullah, A. M. Aldawsari, P. Thounthong and K. S. Nisar, MHD flow and heat transfer in Sodium Alginate fluid with thermal radiation and porosity effects: fractional model of atangana– baleanu derivative of non-local and non-singular kernel, *Symmetry*, **11**(10), 1295 (2019).

[2] F. S. Bayones, A. M. Abd-Alla and E. N. Thabet, Effect of Heat and Mass Transfer and Magnetic Field on Peristaltic Flow of a Fractional Maxwell Fluid in a Tube, *Complexity*, **2021,** 9911820, (2021).

[3] A.M. Abd-Alla, S.M. Abo-Dahab, M.A. Abdelhafez and E.N. Thabet, Effects of heat transfer and the endoscope on Jeffrey fluid peristaltic flow in tubes, *Multidiscip. Model. Mater. Struct.* **17**(5) 895-941 (2021).

[4] M. I. Asjad, M. Aleem, A. Ahmadian, S. Salahshour and M. Ferrara, New trends of fractional modeling and heat and mass transfer investigation of (SWCNTs and MWCNTs)-CMC based nanofluids flow over

inclined plate with generalized boundary conditions, *Chinese Journal of Physics,* **66**, 497-516 (2020).

[5] F. Mainardi and G. Spada, Creep, relaxation and viscosity properties for basic fractional models in rheology, The European Physical Journal Special, 193, 133–160 (2011).

[6] H. Qi and H. Jin, Unsteady rotating flows of a viscoelastic fluid with the fractional Maxwell model between coaxial cylinders, Acta *Mechanica Sinica*, **22**(4), 301–305 (2006).

[7] E. U. Haque, A. U. Awan, N. Raza, M. Abdullah and M. A. Chaudhry, computational approach for the unsteady flow of maxwell fluid with Caputo fractional derivatives, *Alexandria Engineering Journal,* **57**(4), 2601–2608 (2018).

[8] Y.Carrera, G.Avila-de la Rosa, E.J.Vernon-Carter and J.Alvarez-Ramirez, A fractional-order Maxwell model for non-Newtonian fluids, *Physica A: Statistical Mechanics and its Applications,* **482**, 276-285 (2017).

[9] D. Tripathi, S.K. Pandey, S. Das, Peristaltic flow of viscoelastic fluid with fractional Maxwell model through a channel, *Applied Mathematics and Computation*, **215,** 3645–3654, (2010).

[10] X. Guo, J. Zhou, H. Xie and Z. Jiang, MHD Peristaltic Flow of Fractional Jeffrey Model through Porous Medium, *Mathematical Problems in Engineering,* (2018).

[11] D. Tripathi, Peristaltic transport of a viscoelastic fluid in a channel, *Acta Astronautica*, **68**, 1379–1385 (2011).

[12] A.M. Abd-Alla, S.M. Abo-Dahab, M.A. Abdelhafez and E.N. Thabet, Peristaltic pump with heat and mass transfer of a fractional second grade fluid through porous medium inside a tube, *Sci. Rep.* **12**(1), 10608, (2022).

[13] X. Guo and H. Qi, Analytical Solution of Electro-Osmotic Peristalsis of Fractional Jeffreys Fluid in a Micro-Channel, *Micromachines,* **8**(341), (2017).

[14] V. K. Narla, K. M. Prasad and J. V. Ramanamurthy, Peristaltic Motion ofViscoelastic Fluid with Fractional Second Grade Model in Curved Channels, *Chinese Journal of Engineering,* (2013).

[15] A. Razzaq, A. R. Seadawy and N. Raza, Heat transfer analysis of viscoelastic fluid flow with fractional Maxwell model in the cylindrical geometry, *Physica Scripta,* **95**(11), (2020).

[16] K. Javid, S. Ud-Din Khan, S. Ud-Din Khan, M. Hassan, A, Khan and S. A. Alharbi, Mathematical modeling of magneto-peristaltic propulsion of a viscoelastic fluid through a complex wavy non-uniform channel: an application of hall device in bio-engineering domains, *The European Physical Journal Plus,* **136**(182), (2021).

[17] K.Ramesh, D.Tripathib, M. M. Bhatti and C.M. Khalique, Electro-osmotic flow of hydromagnetic dusty viscoelastic fluids in a microchannel propagated by peristalsis, *Journal of Molecular Liquids,* **314**, 113568, (2020).

[18] A.M. Abd-Alla, S.M. Abo-Dahab, M.A. Abdelhafez and E.N. Thabet, Impact of inclined magnetic field on peristaltic flow of blood fluid in an inclined asymmetric channel in the presence of heat and mass transfer, *Waves in Random and Complex Media,* (2022), 10.1080/17455030.2022.2084653.

[19] Z. Khan, H. Ur Rasheed, S. Islam, S. Noor, I. Khan, T. Abbas, W.s Khan, A. H. Seikh, El. M. Sherif and K. S. Nisar, Heat Transfer Effect on Viscoelastic Fluid Used as a Coating Material for Wire with Variable Viscosity, *Coatings*, **10**(2), 163, (2020).

[20] A. M. Abd-Alla, E. N. Thabet and F. S. Bayones, Numerical solution for MHD peristaltic transport in an inclined nanofluid symmetric channel with porous medium, *Sci. Rep.* **12,** 3348, (2022).

[21] K. Javid, U. F. Alqsair, M.Hassan, M. M. Bhatti, T. Ahmad and E.Bobescu, Cilia-assisted flow of viscoelastic fluid in a divergent channel under porosity effects, *Biomechanics and Modeling in Mechanobiology,* (2021).

[22] T. Hayat, F. Bibi, S. Farooq and A. A. Khan, Nonlinear radiative peristaltic flow of Jeffrey nanofluid with activation energy and modified Darcy's law, *Journal of the Brazilian Society of Mechanical Sciences and Engineering*, **41**, 296, (2019).

[23] F. S. Bayones, A. M. Abd-Alla and E. N. Thabet, Magnetized dissipative Soret effect on nonlinear radiative Maxwell nanofluid flow with porosity, chemical reaction and Joule heating, *Waves in Random and Complex Media*, (2022), 10.1080/17455030.2021.2019352.

[24] M. Kothandapani and S. Srinivas, On the influence of wall properties in the MHD peristaltic transport with heat transfer and porous medium, *Physcis Letter A,* **372** (25), 4586–4591 (2008).

[25] K. Vajravelu, G. Radhakrishnamacharya and V. Radha Krishnamurty, Peristaltic flow and heat transfer in a vertical porous annulus, with long wave approximation, *International Journal of Non-Linear Mechanics,* **42**(5), 754–759 (2007).